Structural Engineering and Mechanics, *Vol. 64, No. 1 (2017) 81-92*
DOI: https://doi.org/10.12989/sem.2017.64.1.081

Analytical and numerical study of temperature stress in the bi-modulus thick cylinder

Jinling Gao[*1], Peikui Huang[2a] and Wenjuan Yao[3b]

[1]*School of Aeronautics and Astronautics, Purdue University, West Lafayette, IN 47907, USA*
[2]*College of Engineering, South China Agricultural University, Guangzhou 510642, China*
[3]*Department of Civil Engineering, Shanghai University, Shanghai 200444, China*

(Received August 23, 2016, Revised June 6, 2017, Accepted July 12, 2017)

Abstract. Many materials in engineering exhibit different modulus in tension and compression, which are known as bi-modulus materials. Based on the bi-modulus elastic theory, a modified semi-analytical model, by introducing a stress function, is established in this paper to study the mechanical response of a bi-modulus cylinder placed in an axisymmetric temperature field. Meanwhile, a numerical procedure to calculate the temperature stresses in bi-modulus structures is developed. It is proved that the bi-modulus solution can be degenerated to the classical same modulus solution, and is in great accordance with the solutions calculated by the semi-analytical model proposed by Kamiya (1977) and the numerical solutions calculated both by the procedure complied in this paper and by the finite element software ABAQUS, which demonstrates that the semi-analytical model and the numerical procedure are accurate and reliable. The result shows that the modified semi-analytical model simplifies the calculation process and improves the speed of computation. And the numerical procedure simplifies the modeling process and can be extended to study the stress field of bi-modulus structures with complex geometry and boundary conditions. Besides, the necessity to introduce the bi-modulus theory is discussed and some suggestions for the qualitative analysis and the quantitative calculation of such structure are proposed.

Keywords: bi-modulus thick cylinder; axisymmetric temperature field; stress function; semi-analytical solution; numerical procedure

1. Introduction

Thick cylinder shows a broaden application in engineering, such as civil engineering, petroleum engineering, nuclear engineering, mechanical engineering. Previous researches on such structure are mostly based on the classical same modulus theory, which argues that materials show only one elastic modulus in tension and compression (Chandrashekhara and Bhimaraddi 1982, Zhou 1981). However, various experiments indicate that many materials in engineering have different tensile modulus and compressive modulus, such as concrete (Guo and Zhang 1987), nuclear graphite (Medri 1982), metal alloy (Gilbert 1961), biological materials (Cai and Qin 2014), polymer and composite (Bertoldi *et al*. 2008, Patel *et al*. 2014), and so on. Particularly, graphene, the thinnest but hardest material with minimum electrical resistivity does have higher compressive modulus than tensile modulus (Tsoukleri and Parthenios 2009, Geim 2009). For a structure composed of such materials, elastic coefficients not only depend on the structural material, but also change with displacement and stress state of a certain point in the structure, which means they are related to material, geometry, boundary conditions and loads of the structure. The bi-modulus problem is actually a kind of non-linear problem caused by many factors. If the classical same modulus theory is still adopted, a significant error may generate in the structural calculation and design. Therefore, the bi-modulus theory is proposed to accomplish accurate analyses, excavate the potential of materials and invent novel materials, which is always a hot studying topic.

Timoshenko (1994) proposed the concept of bi-modulus materials when he studied the mechanical behavior of a pure bending beam. Afterwards, the constitutive model, the finite element method and the analytical method of the bi-modulus theory were put forward and applied to practical engineering.

According to the combination of principal stresses with different signs, Ambartsumyan (1965) divided a structure into two kinds of region: (1) tensile region with three principle stresses being uniformly positive or compressive region with three principle stresses being all negative; (2) complex stress region with three principle stresses having different signs. The elastic matrix and the interface between tensile region and compressive region are key problems in the study on the constitutive model of bi-modulus materials. Ambartsumyan raised the bi-linear model to describe the stress-strain relation of a bi-modulus material. He also argued that the coefficients in the flexibility matrix were determined according to the sign of each principle stress. According to the sign of the first stress invariant, Shapiro (1971) proposed another criterion to obtain the flexibility

∗Corresponding author, Ph.D. Student
E-mail: gao468@purdue.edu
[a]Ph.D. Student
[b]Professor

http://www.techno-press.com/journals/sem&subpage=7 ISSN: 1225-4568 (Print), 1598-6217 (Online)

matrix. Considering the Poisson's effect, Jones (1971) introduced the average value and the weighting coefficient to get coefficients out of the leading diagonal of matrix and established two modified models. Vijayakumar (1990) put forward that the computational model may be separated into some small sub-matrices and then the tensile region and the compressive region may be divided into more tiny zones. Green, Mkrtichian (1977), Ye (2001) suggested that material properties may more rely on the sign of strain comparing to stress and then they developed the principal strain model.

In the early times, the finite element method (FEM) is widely used to solve bi-modulus problems. Until now, five main methods are suggested to improve the precision and the speed of calculation, including the initial stress method raised by Yang *et al*. (1992) , a modified method through introducing an accelerating convergence factor and a general formula to calculate the shear elastic modulus put forward by Zhang and Wang (1989), Liu and Zhang (2002), Liu and Meng (2002), a simplified model adopted the principle of $\mu t/Et=\mu c/Ec$ presented by Ye (1997), the smoothing function method proposed by Yang and Zhu (2006) and the method by introducing different shear modulus in tension and compression proposed by He *et al*. (2009).

Superior to FEM, the analytical method enables researchers to easily get the stress field and deformation field of structures and execute the qualitative sensitive parameters analysis. Ambartsumyan (1965) derived the analytical expressions of stresses and deformation of various bi-modulus structures subjected to simple loads. Based on the plane cross-section assumption, Yao and Ye (2004a) proved that the position of the neutral layer in a bi-modulus structure has no relationship with the shear stress. And then some analytical or semi-analytical models are established to study the mechanical behavior of bi-modulus structures in engineering, like bending beams (Yao and Ye 2004a), bending-compression columns (Yao and Ye 2004b), statically indeterminate structures (Yao and Ye 2006a), composite structures (Yao *et al*. 2006b) and compression rods with small deflection (Yao and Ma 2013) and large deflection (Yao *et al*. 2015). By introducing the simplified equivalent cross-section method, He *et al* (2007, 2010a, 2010b, 2012, 2015) deduced the analytical solution of bi-modulus bending beams, bi-modulus bending-compression columns, bi-modulus thin plates, bi-modulus plates with the large deflection and bi-modulus curve beams. Leal *et al*. (2009) gave the compressive strength equation of high performance fiber with different modulus in tension and compression. Wu *et al*. (2010) studied the bending of bi-modulus plates with large deflection. Shi and Gao (2015) realize the application of the bi-modulus theory in the structural topology optimization technology.

By now, few researches have been conducted to study the mechanical response of bi-modulus structures placed in the axisymmetric temperature field. Kamiya (1977) deduced the displacement governing equation of the bi-modulus cylinder under the axisymmetric temperature field. However, the semi-analytical model established by Kamiya (1977) is very complex with eight non-linear equations to be solved and cannot be applied to the analysis and calculation of structures with slightly higher computational accuracy in practical engineering (Li *et al*. 2008, Fang *et al*. 2014). In view of this, a stress function is introduced in this paper to simplify Kamiya's model and accomplish the precise analysis of the mechanical response of a bi-modulus thick cylinder under the axisymmetric temperature field. Meanwhile, numerical studies are conducted, including developing a FEM procedure and the ABAQUS simulation. Finally, the calculation discrepancy between the bi-modulus solution and the classical same modulus solution is discussed.

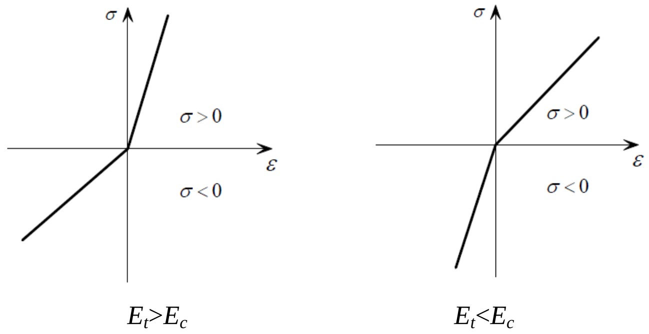

Fig. 1 Constitutive model for bi-modulus materials (bi-linear model)

2. Mechanical model

2.1 Basic concept

In this paper, the bi-linear model proposed by Ambartsumyan (1965) is adopted to describe the stress-strain relationship of a bi-modulus material, which is shown in Fig. 1. It means that a material may generate the corresponding tensile strain and compressive strain with different absolute values when it is subjected to tensile stress and compressive stress with the same absolute value. Therefore, the material has a tensile modulus E_t and another compressive modulus E_c with different magnitudes. In the meantime, the Poisson's ratio of a bi-modulus material meets the equation $-\frac{\mu_t}{E_t}=-\frac{\mu_c}{E_c}$, where μ_t and μ_c are the tensile Poisson's ratio and the compressive Poisson's ratio, respectively.

2.2 Assumption

The bi-modulus cylinder studied in this paper meets some basic assumptions in mechanics of elasticity, including a solid, continuity, homogeneity and isotropy. In addition, merely small deformation will happen during the whole loading process. Therefore, the difference of the bi-modulus theory with the classical same modulus theory is only reflected in the constitutive equations but the equilibrium equations, geometric equations and deformation continuity equations are all the same. The material will

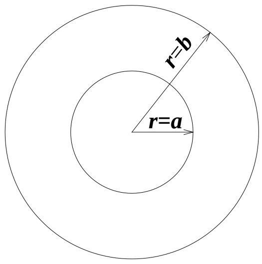

Fig. 2 Structural model

show different elastic properties (E_c, E_t, μ_c, μ_t) according to different signs of principal stresses.

2.3 Structural model

As shown in Fig. 2, an infinite cylinder, with the inner diameter *a* and the external diameter *b*, is made of the bi-modulus material. The tensile elastic modulus and the compressive elastic modulus are E_t and E_c, respectively. Correspondingly, the Poisson's rations in tension and compression are μ_t and μ_c. The coefficient of thermal expansion is α. A polar coordinate system O-$r\theta z$ with the origin set on the center of a circle is established.

The cylinder is placed in the axisymmetric temperature field $T=T(r)$ and the temperature is distributed uniformly along the longitudinal direction.

3. Theoretical analysis and analytical derivation

3.1 Establishment of governing equation of stress function

According to the theory of elasticity, the strain components in principal directions can be described as

$$\varepsilon_{rr} = a_{11}\sigma_{rr} + a_{12}\sigma_{\theta\theta} + a_{13}\sigma_{zz} + \alpha T \tag{1a}$$

$$\varepsilon_{\theta\theta} = a_{21}\sigma_{rr} + a_{22}\sigma_{\theta\theta} + a_{23}\sigma_{zz} + \alpha T \tag{1b}$$

$$\varepsilon_{zz} = a_{31}\sigma_{rr} + a_{32}\sigma_{\theta\theta} + a_{33}\sigma_{zz} + \alpha T \tag{1c}$$

where

$$a_{11} = \begin{cases} a_{11}^t = 1/E_t\left(\sigma_{rr} > 0\right) \\ a_{11}^c = 1/E_c\left(\sigma_{rr} < 0\right) \end{cases},$$

$$a_{22} = \begin{cases} a_{22}^t = 1/E_t\left(\sigma_{\theta\theta} > 0\right) \\ a_{22}^c = 1/E_c\left(\sigma_{\theta\theta} < 0\right) \end{cases},$$

$$a_{33} = \begin{cases} a_{33}^t = 1/E_t\left(\sigma_{zz} > 0\right) \\ a_{33}^c = 1/E_c\left(\sigma_{zz} < 0\right) \end{cases}.$$

It is assumed that $-\dfrac{\mu_t}{E_t} = -\dfrac{\mu_c}{E_c}$. Then we can get $a_{12} = a_{21} = a_{13} = a_{31} = a_{23} = a_{32} = -\dfrac{\mu_t}{E_t} = -\dfrac{\mu_c}{E_c}$.

Mechanical analysis of the infinite cylinder is regarded as a kind of plane strain problem. Then we have

$$\varepsilon_{zz} = 0 \tag{2}$$

Combine Eq. (1) and Eq. (2), we have

$$\varepsilon_{rr} = b_{11}\sigma_{rr} + b_{12}\sigma_{\theta\theta} + b_\alpha T \tag{3a}$$

$$\varepsilon_{\theta\theta} = b_{21}\sigma_{rr} + b_{22}\sigma_{\theta\theta} + b_\alpha T \tag{3b}$$

where the elastic coefficients are

$$b_{11} = \frac{a_{11}a_{33} - a_{12}^2}{a_{33}},\quad b_{22} = \frac{a_{22}a_{33} - a_{12}^2}{a_{33}},$$

$$b_{12} = b_{21} = a_{12}\left(1 - \frac{a_{12}}{a_{33}}\right),\quad b_\alpha = \alpha\left(1 - \frac{a_{12}}{a_{33}}\right)$$

For axisymmetric problems, the geometric equations can be simplified as

$$\varepsilon_{rr} = \frac{\partial u_{rr}}{\partial r} \tag{4a}$$

$$\varepsilon_{\theta\theta} = \frac{u_{rr}}{r} \tag{4b}$$

$$\tau_{r\theta} = 0 \tag{4c}$$

According to Eq. (4), the continuity equation of strain is obtained as

$$r\frac{d\varepsilon_{\theta\theta}}{dr} + \varepsilon_{\theta\theta} - \varepsilon_{rr} = 0 \tag{5}$$

Considering the axial symmetry, the equilibrium equation can be written as

$$r\frac{d\sigma_{rr}}{dr} + \sigma_{rr} - \sigma_{\theta\theta} = 0 \tag{6}$$

where the radial stress σ_{rr} and the circumferential stress $\sigma_{\theta\theta}$ are the principal stresses unrelated to θ and are actually the function of r. Now we introduce the stress function $\psi(r)$ to substitute the principle stresses as

$$\sigma_{rr} = \frac{\psi}{r} \tag{7a}$$

$$\sigma_{\theta\theta} = \frac{d\psi}{dr} \tag{7b}$$

For the plane strain problem, we have

$$\sigma_{zz} = \begin{cases} \mu_t\left(\sigma_{rr} + \sigma_{\theta\theta}\right) - \alpha E_t T & \sigma_{zz} > 0 \\ \mu_c\left(\sigma_{rr} + \sigma_{\theta\theta}\right) - \alpha E_c T & \sigma_{zz} < 0 \end{cases} \tag{8}$$

Substituting Eq. (7) into Eq. (3) and then into Eq. (5) with considering Eq. (6) simultaneously, the governing equation of stress function can be gained as

$$r^2\frac{d^2\psi}{dr^2} + r\frac{d\psi}{dr} - \frac{b_{11}}{b_{22}}\psi + \frac{b_\alpha}{b_{22}}r^2\frac{dT}{dr} = 0 \tag{9}$$

3.2 Derivation of stress expression with unknown parameters

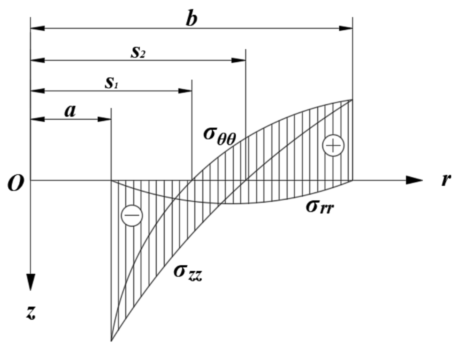

Fig. 3 Stress distribution in the cylinder using the classical same modulus theory

Taking a steady temperature field as an example, the analytical expressions of stresses of the bi-modulus cylinder can be deduced. It is assumed that the temperature at the inner wall is T_0>0 and that at the outer wall is 0. The equation of heat conduction can be described as

$$\frac{1}{r}\frac{d}{dr}\left(r\frac{dT}{dr}\right)=0 \tag{10}$$

where the boundary conditions are

$$\text{when } r=a,\ T=T_0 \tag{11a}$$

$$\text{when } r=b,\ T=0 \tag{11b}$$

Considering the steady heat flow, the temperature function will be

$$T=T_0\frac{\ln\left(b/r\right)}{\ln\left(b/a\right)} \tag{12}$$

For the classical same modulus problem, in such working condition, the radial stress is compressive. That is to say, σ_{rr}<0 appears at the random point of the cylinder. The circumferential stress $\sigma_{\theta\theta}$ and the axial stress σ_{zz} are the continuous function of coordinate r and are negative at the inner wall and positive at the outer wall. The stress distribution in the cylinder is shown as Fig. 3.

For bi-modulus materials, the stress distribution is similar to the classical same modulus solution (Kamiya 1977). Therefore, we have σ_{rr}<0 and the signs of both the circumferential stress and the axial stress change with the increase of radius r. It is assumed that $\sigma_{\theta\theta}$=0 when r=s_1, and σ_{zz}=0 when r=s_2, where $a<s_1<s_2<b$.

Consequently, the random cross section of the cylinder can be divided into three regions:

1. When $a<r<s_1$, we have $\sigma_{rr}<0$, $\sigma_{\theta\theta}<0$, $\sigma_{zz}<0$
2. When $s_1<r<s_2$, we have $\sigma_{rr}<0$, $\sigma_{\theta\theta}>0$, $\sigma_{zz}<0$
3. When $s_2<r<b$, we have $\sigma_{rr}<0$, $\sigma_{\theta\theta}>0$, $\sigma_{zz}>0$

For the first region $a<r<s_1$, we have σ_{rr}<0, $\sigma_{\theta\theta}$<0, σ_{rr}<0 and then we have

$$b_{11}^a=b_{22}^a=\frac{1}{E_c}\left(1-\mu_c^2\right),\quad b_{12}^a=-\frac{\mu_c\left(1+\mu_c\right)}{E_c},\quad b_\alpha^a=\alpha\left(1+\mu_c\right)$$

Define $k_1=\sqrt{\dfrac{b_{11}^a}{b_{22}^a}}=1$

The governing equation of the stress function can be simplified as

$$r^2\frac{d^2\psi}{dr^2}+r\frac{d\psi}{dr}-\psi-\frac{b_\alpha^a}{b_{22}^a}\frac{T_0 r}{\ln\left(b/a\right)}=0 \tag{13}$$

Solving Eq. (13), the expression of the stress function can be written as

$$\psi\left(r\right)=C_1 r+\frac{C_2}{r}+\frac{b_\alpha^a}{2b_{22}^a}\frac{T_0}{\ln\left(b/a\right)}r\ln r \tag{14}$$

where C_1 and C_2 are both the unknown parameters having no relationship with the radius r.

Substituting Eq. (14) into Eq. (7), the radial stress σ_{rr} and the circumferential stress $\sigma_{\theta\theta}$ can be obtained as

$$\sigma_{rr}=C_1+\frac{C_2}{r^2}+\frac{b_\alpha^a}{2b_{22}^a}\frac{T_0}{\ln\left(b/a\right)}\ln r \tag{15a}$$

$$\sigma_{\theta\theta}=C_1-\frac{C_2}{r^2}+\frac{b_\alpha^a}{2b_{22}^a}\frac{T_0}{\ln\left(b/a\right)}\left(1+\ln r\right) \tag{15b}$$

According to Eq. (8), we can get

$$\sigma_{zz}=\mu_c\left[2C_1+\frac{b_\alpha^a}{2b_{22}^a}\frac{T_0}{\ln\left(b/a\right)}\left(1+2\ln r\right)\right]-E_c\alpha T_0\frac{\ln\left(b/r\right)}{\ln\left(b/a\right)} \tag{15c}$$

Analogously, for the second region $s_1<r<s_2$, the expression of the stress function can be written as

$$\psi\left(r\right)=C_3 r^{k_2}+C_4 r^{-k_2}+\frac{b_\alpha^b}{b_{22}^b}\frac{T_0}{\ln\left(b/a\right)}\frac{r}{1-k_2^2} \tag{16}$$

The expressions of three principle stresses can be gained as

$$\sigma_{rr}=C_3 r^{k_2-1}+C_4 r^{-\left(k_2+1\right)}+\frac{b_\alpha^b}{b_{22}^b}\frac{T_0}{\ln\left(b/a\right)}\frac{1}{1-k_2^2} \tag{17a}$$

$$\sigma_{\theta\theta}=C_3 k_2 r^{k_2-1}-C_4 k_2 r^{-\left(k_2+1\right)}+\frac{b_\alpha^b}{b_{22}^b}\frac{T_0}{\ln\left(b/a\right)}\frac{1}{1-k_2^2} \tag{17b}$$

$$\begin{aligned}\sigma_{zz}=\mu_c\Big[&\left(1+k_2\right)C_3 r^{k_2-1}+\left(1-k_2\right)C_4 r^{-\left(k_2+1\right)}\\&+\frac{b_\alpha^b}{b_{22}^b}\frac{T_0}{\ln\left(b/a\right)}\frac{2}{1-k_2^2}\Big]-E_c\alpha T_0\frac{\ln\left(b/r\right)}{\ln\left(b/a\right)}\end{aligned} \tag{17c}$$

where

$$b_{11}^b=\frac{1}{E_c}\left(1-\mu_c^2\right),\quad b_{22}^b=\frac{1}{E_t}\left(1-\mu_t^2\right),\quad b_{12}^b=-\frac{\mu_c\left(1+\mu_c\right)}{E_c},$$

$$b_\alpha^b=\alpha\left(1+\mu_c\right),\ k_2=\sqrt{\frac{b_{11}^b}{b_{22}^b}}=\sqrt{\frac{E_t}{E_c}\frac{\left(1-\mu_c^2\right)}{\left(1-\mu_t^2\right)}}$$

C_3 and C_4 are both the unknown parameters unrelated to the radius r.

And for the third region $s_2<r<b$, we have the stress function

$$\psi\left(r\right)=C_5 r^{k_3}+C_6 r^{-k_3}+\frac{b_\alpha^c}{b_{22}^c}\frac{T_0}{\ln\left(b/a\right)}\frac{r}{1-k_3^2} \tag{18}$$

And the stress can be described as

$$\sigma_{rr}=C_5 r^{k_3-1}+C_6 r^{-(k_3+1)}+\frac{b_\alpha^c}{b_{22}^c}\frac{T_0}{\ln(b/a)}\frac{1}{1-k_3^2} \tag{19a}$$

$$\sigma_{\theta\theta}=C_5 k_3 r^{k_3-1}-C_6 k_3 r^{-(k_3+1)}+\frac{b_\alpha^c}{b_{22}^c}\frac{T_0}{\ln(b/a)}\frac{1}{1-k_3^2} \tag{19b}$$

$$\begin{aligned}\sigma_{zz}=\mu_t\Big[&(1+k_3)C_5 r^{k_3-1}+(1-k_3)C_6 r^{-(k_3+1)}\\ &+\frac{b_\alpha^c}{b_{22}^c}\frac{T_0}{\ln(b/a)}\frac{2}{1-k_3^2}\Big]-E_t\alpha T_0\frac{\ln(b/r)}{\ln(b/a)}\end{aligned} \tag{19c}$$

where

$b_{11}^c=\frac{1}{E_c}\left(1-\mu_c^2\right)$, $b_{22}^c=\frac{1}{E_t}\left(1-\mu_t^2\right)$, $b_{12}^c=-\frac{\mu_t(1+\mu_t)}{E_t}$,

$b_\alpha^c=\alpha(1+\mu_t)$, $k_3=\sqrt{\frac{b_{11}^c}{b_{22}^c}}=\sqrt{\frac{E_t}{E_c}\frac{\left(1-\mu_c^2\right)}{\left(1-\mu_t^2\right)}}$

C_5 and C_6 are both the unknown parameters independent of the radius r.

3.3 Parameter solving of stress expression

The boundary conditions of three regions are as follows

$$\text{when } r=a,\ \sigma_{rr}=0 \tag{20a}$$

$$\text{when } r=s_1,\ \sigma_{\theta\theta}^-=0 \tag{20b}$$

$$\text{when } r=s_1,\ \sigma_{\theta\theta}^+=0 \tag{20c}$$

$$\text{when } r=s_2,\ \sigma_{zz}^-=0 \tag{20d}$$

$$\text{when } r=s_2,\ \sigma_{zz}^+=0 \tag{20e}$$

$$\text{when } r=b,\ \sigma_{rr}=0 \tag{20f}$$

Substituting the corresponding stress expressions into the above boundary condition expressions, the unknown parameters in the expressions of stresses can be solved as

$$C_1=-\frac{b_\alpha^a}{2b_{22}^a}\frac{T_0}{\ln(b/a)}\left[\frac{s_1^2}{a^2+s_1^2}\left(1-\ln\frac{a}{s_1}\right)+\ln a\right] \tag{21a}$$

$$C_2=\frac{b_\alpha^a}{2b_{22}^a}\frac{T_0}{\ln(b/a)}\frac{a^2 s_1^2}{a^2+s_1^2}\left(1-\ln\frac{a}{s_1}\right) \tag{21b}$$

$$\begin{aligned}C_3=&-\frac{b_\alpha^b}{b_{22}^b}\frac{T_0}{\ln(b/a)}\frac{1}{1-k_2^2}\frac{1}{k_2}\frac{(1-k_2)s_1^{k_2+1}+2k_2 s_2^{k_2+1}}{(1+k_2)s_2^{2k_2}+(1-k_2)s_1^{2k_2}}+\\ &\frac{E_c\alpha T_0}{\mu_c}\frac{\ln(b/s_2)}{\ln(b/a)}\frac{s_1^{-(k_2+1)}}{(1+k_2)s_1^{-(k_2+1)}s_2^{k_2-1}+(1-k_2)s_1^{k_2-1}s_2^{-(k_2+1)}}\end{aligned} \tag{21c}$$

$$\begin{aligned}C_4=&\frac{b_\alpha^b}{b_{22}^b}\frac{T_0}{\ln(b/a)}\frac{1}{1-k_2^2}\frac{1}{k_2}\frac{(1+k_2)s_1^{k_2+1}s_2^{2k_2}-2k_2 s_1^{2k_2}s_2^{k_2+1}}{(1+k_2)s_2^{2k_2}+(1-k_2)s_1^{2k_2}}+\\ &\frac{E_c\alpha T_0}{\mu_c}\frac{\ln(b/s_2)}{\ln(b/a)}\frac{s_1^{k_2-1}}{(1+k_2)s_1^{-(k_2+1)}s_2^{k_2-1}+(1-k_2)s_1^{k_2-1}s_2^{-(k_2+1)}}\end{aligned} \tag{21d}$$

$$\begin{aligned}C_5=&\frac{b_\alpha^c}{b_{22}^c}\frac{T_0}{\ln(b/a)}\frac{1}{1-k_3^2}\frac{(1-k_3)b^{k_3+1}-2s_2^{k_3+1}}{(1+k_3)s_2^{2k_3}-(1-k_3)b^{2k_3}}+\\ &\frac{E_t\alpha T_0}{\mu_t}\frac{\ln(b/s_2)}{\ln(b/a)}\frac{b^{-(k_3+1)}}{(1+k_3)s_2^{k_3-1}b^{-(k_3+1)}-(1-k_3)s_2^{-(k_3+1)}b^{k_3-1}}\end{aligned} \tag{21e}$$

$$\begin{aligned}C_6=&-\frac{b_\alpha^c}{b_{22}^c}\frac{T_0}{\ln(b/a)}\frac{1}{1-k_3^2}\frac{(1+k_3)s_2^{2k_3}b^{k_3+1}-2s_2^{k_3+1}b^{2k_3}}{(1+k_3)s_2^{2k_3}-(1-k_3)b^{2k_3}}-\\ &\frac{E_t\alpha T_0}{\mu_t}\frac{\ln(b/s_2)}{\ln(b/a)}\frac{b^{k_3-1}}{(1+k_3)s_2^{k_3-1}b^{-(k_3+1)}-(1-k_3)s_2^{-(k_3+1)}b^{k_3-1}}\end{aligned} \tag{21f}$$

Then the stress expressions of random points in the cylinder are as below

when $a<r<s_1$

$$\sigma_{rr}=\frac{b_\alpha^a}{2b_{22}^a}\frac{T_0}{\ln(b/a)}\left[\frac{s_1^2}{a^2+s_1^2}\left(1-\ln\frac{a}{s_1}\right)\left(\frac{a^2}{r^2}-1\right)-\ln\frac{a}{r}\right] \tag{22a}$$

$$\sigma_{\theta\theta}=\frac{b_\alpha^a}{2b_{22}^a}\frac{T_0}{\ln(b/a)}\left[\frac{s_1^2}{a^2+s_1^2}\left(1-\ln\frac{a}{s_1}\right)\left(-\frac{a^2}{r^2}-1\right)+\left(1-\ln\frac{a}{r}\right)\right] \tag{22b}$$

$$\begin{aligned}\sigma_{zz}=\frac{\mu_c b_\alpha^a}{2b_{22}^a}\frac{T_0}{\ln(b/a)}\Big[&-\frac{2s_1^2}{a^2+s_1^2}\left(1-\ln\frac{a}{s_1}\right)\\ &+\left(1-2\ln\frac{a}{r}\right)\Big]-E_c\alpha T_0\frac{\ln(b/r)}{\ln(b/a)}\end{aligned} \tag{22c}$$

when $s_1<r<s_2$

$$\begin{aligned}\sigma_{rr}=&\left\{1+\frac{1}{k_2}\frac{\left[(1+k_2)s_1^{k_2+1}s_2^{2k_2}-2k_2 s_1^{2k_2}s_2^{k_2+1}\right]r^{-(k_2+1)}-\left[(1-k_2)s_1^{k_2+1}+2k_2 s_2^{k_2+1}\right]r^{k_2-1}}{(1+k_2)s_2^{2k_2}+(1-k_2)s_1^{2k_2}}\right\}\\ &\cdot\frac{b_\alpha^b}{b_{22}^b}\frac{T_0}{\ln(b/a)}\frac{1}{1-k_2^2}+\frac{E_c\alpha T_0}{\mu_c}\frac{\ln(b/s_2)}{\ln(b/a)}\frac{s_1^{-(k_2+1)}r^{k_2-1}+s_1^{k_2-1}r^{-(k_2+1)}}{(1+k_2)s_1^{-(k_2+1)}s_2^{k_2-1}+(1-k_2)s_1^{k_2-1}s_2^{-(k_2+1)}}\end{aligned} \tag{22d}$$

$$\begin{aligned}\sigma_{\theta\theta}=&\left\{1-\frac{\left[(1+k_2)s_1^{k_2+1}s_2^{2k_2}-2k_2 s_1^{2k_2}s_2^{k_2+1}\right]r^{-(k_2+1)}+\left[(1-k_2)s_1^{k_2+1}+2k_2 s_2^{k_2+1}\right]r^{k_2-1}}{(1+k_2)s_2^{2k_2}+(1-k_2)s_1^{2k_2}}\right\}\\ &\cdot\frac{b_\alpha^b}{b_{22}^b}\frac{T_0}{\ln(b/a)}\frac{1}{1-k_2^2}+\frac{k_2 E_c\alpha T_0}{\mu_c}\frac{\ln(b/s_2)}{\ln(b/a)}\frac{s_1^{-(k_2+1)}r^{k_2-1}-s_1^{k_2-1}r^{-(k_2+1)}}{(1+k_2)s_1^{-(k_2+1)}s_2^{k_2-1}+(1-k_2)s_1^{k_2-1}s_2^{-(k_2+1)}}\end{aligned} \tag{22e}$$

$$\begin{aligned}\sigma_{zz}=&\left\{\frac{1}{k_2}\frac{\left[(1+k_2)s_1^{k_2+1}s_2^{2k_2}-2k_2 s_1^{2k_2}s_2^{k_2+1}\right](1-k_2)r^{-(k_2+1)}-\left[(1-k_2)s_1^{k_2+1}+2k_2 s_2^{k_2+1}\right](1+k_2)r^{k_2-1}}{(1+k_2)s_2^{2k_2}+(1-k_2)s_1^{2k_2}}\right.\\ &\left.+2\right\}\frac{b_\alpha^b}{b_{22}^b}\frac{T_0}{\ln(b/a)}\frac{\mu_c}{1-k_2^2}+E_c\alpha T_0\frac{\ln(b/s_2)}{\ln(b/a)}\frac{(1+k_2)s_1^{-(k_2+1)}r^{k_2-1}+(1-k_2)s_1^{k_2-1}r^{-(k_2+1)}}{(1+k_2)s_1^{-(k_2+1)}s_2^{k_2-1}+(1-k_2)s_1^{k_2-1}s_2^{-(k_2+1)}}-E_c\alpha T_0\frac{\ln(b/r)}{\ln(b/a)}\end{aligned} \tag{22f}$$

when $s_2<r<b$

$$\begin{aligned}\sigma_{rr}=&\left\{1+\frac{\left[(1-k_3)b^{k_3+1}-2s_2^{k_3+1}\right]r^{k_3-1}-\left[(1+k_3)s_2^{2k_3}b^{k_3+1}-2s_2^{k_3+1}b^{2k_3}\right]r^{-(k_3+1)}}{(1+k_3)s_2^{2k_3}-(1-k_3)b^{2k_3}}\right\}\\ &\cdot\frac{b_\alpha^c}{b_{22}^c}\frac{T_0}{\ln(b/a)}\frac{1}{1-k_3^2}+\frac{E_t\alpha T_0}{\mu_t}\frac{\ln(b/s_2)}{\ln(b/a)}\frac{b^{-(k_3+1)}r^{k_3-1}-b^{k_3-1}r^{-(k_3+1)}}{(1+k_3)s_2^{k_3-1}b^{-(k_3+1)}-(1-k_3)s_2^{-(k_3+1)}b^{k_3-1}}\end{aligned} \tag{22g}$$

$$\sigma_{\theta\theta}=\left\{1+k_3\cdot\frac{\left[(1-k_3)b^{k_3+1}-2s_2^{k_3+1}\right]r^{k_3-1}+\left[(1+k_3)s_2^{2k_3}b^{k_3+1}-2s_2^{k_3+1}b^{2k_3}\right]r^{-(k_3+1)}}{(1+k_3)s_2^{2k_3}-(1-k_3)b^{2k_3}}\right\}$$
$$\cdot\frac{b_\alpha^c}{b_{22}^c}\frac{T_0}{\ln(b/a)}\frac{1}{1-k_3^2}+\frac{k_3E_t\alpha T_0}{\mu_t}\frac{\ln(b/s_2)}{\ln(b/a)}\frac{b^{-(k_3+1)}r^{k_3-1}+b^{k_3-1}r^{-(k_3+1)}}{(1+k_3)s_2^{k_3-1}b^{-(k_3+1)}-(1-k_3)s_2^{-(k_3+1)}b^{k_3-1}} \tag{22f}$$

$$\sigma_{zz}=\left\{2+\frac{\left[(1-k_3)b^{k_3+1}-2s_2^{k_3+1}\right](1+k_3)r^{k_3-1}-\left[(1+k_3)s_2^{2k_3}b^{k_3+1}-2s_2^{k_3+1}b^{2k_3}\right](1-k_3)r^{-(k_3+1)}}{(1+k_3)s_2^{2k_3}-(1-k_3)b^{2k_3}}\right\}$$
$$\cdot\frac{b_\alpha^b}{b_{22}^b}\frac{T_0}{\ln(b/a)}\frac{\mu_t}{1-k_3^2}+E_t\alpha T_0\frac{\ln(b/s_2)}{\ln(b/a)}\frac{(1+k_3)b^{-(k_3+1)}r^{k_3-1}-(1-k_3)b^{k_3-1}r^{-(k_3+1)}}{(1+k_3)b^{-(k_3+1)}s_2^{k_3-1}-(1-k_3)b^{k_3-1}s_2^{-(k_2+1)}}-E_t\alpha T_0\frac{\ln(b/r)}{\ln(b/a)} \tag{22i}$$

$$\frac{b_\alpha^b}{b_{22}^b}\frac{1}{1-k_2^2}\left\{1+\frac{1}{k_2}\frac{(1+k_2)s_2^{2k_2}-(1-k_2)s_1^{2k_2}-4k_2s_1^{k_2-1}s_2^{k_2+1}}{(1+k_2)s_2^{2k_2}+(1-k_2)s_1^{2k_2}}\right\}+\frac{2E_c\alpha\ln(b/s_2)}{\mu_c}$$
$$\cdot\frac{1}{\left[(1+k_2)\left(\frac{s_2}{s_1}\right)^{k_2-1}+(1-k_2)\left(\frac{s_1}{s_2}\right)^{k_2+1}\right]}=\frac{b_\alpha^a}{2b_{22}^a}\left[\frac{a^2-s_1^2}{a^2+s_1^2}\left(1-\ln\frac{a}{s_1}\right)-\ln\frac{a}{s_1}\right] \tag{24a}$$

$$\left\{\frac{b_\alpha^b}{b_{22}^b}\left[1+\frac{2s_2^{k_2-1}s_1^{k_2+1}-2s_1^{2k_2}-2s_2^{2k_2}}{(1+k_2)s_2^{2k_2}+(1-k_2)s_1^{2k_2}}\right]-\frac{b_\alpha^c}{b_{22}^c}\left[1+\frac{-2k_3s_2^{k_3-1}b^{k_3+1}-2s_2^{2k_3}+2b^{2k_3}}{(1+k_3)s_2^{2k_3}-(1-k_3)b^{2k_3}}\right]\right\}\cdot$$
$$\frac{1}{1-k_2^2}=\frac{E_t\alpha\ln(b/s_2)}{\mu_t}\left[\frac{s_2^{2k_3}-b^{2k_3}}{(1+k_3)s_2^{2k_3}-(1-k_3)b^{2k_3}}-\frac{s_2^{2k_2}+s_1^{2k_2}}{(1+k_2)s_2^{2k_2}+(1-k_2)s_1^{2k_2}}\right] \tag{24b}$$

3.3 Governing equation set of radii of curvature of the neutral layer

On the interface of different regions, continuity conditions of stress should be satisfied, which are

$$\text{when}\quad r=s_1 \text{ or } r=s_2\,,\quad \sigma_{rr}^-=\sigma_{rr}^+ \tag{23}$$

Substitute Eq. (22*a*), Eq. (22*b*) and Eq. (22*g*) respectively into Eq. (23) and then we can get the simplified transcendental equation set about s_1 and s_2 as Eq. (24a) and Eq. (24b).

A non-linear iteration procedure based on Newton's method is developed on MATLAB platform to gain the solutions of the equation set Eq. (24). It's worth noting that s_1 and s_2 are both limited to the range from a=1.5 to b=2.5. Rational initial values are chosen and substituted into the procedure. Numerical solutions of s_1 and s_2 are obtained. The calculation flow chart is shown as Fig. 4.

Substituting s_1 and s_2 into Eq. (21), we have the expressions of stresses. According to Eq. (1), the expressions of strains can be obtained. Finally, the expressions of displacements can be deduced by substituting the expressions of strains into Eq. (4).

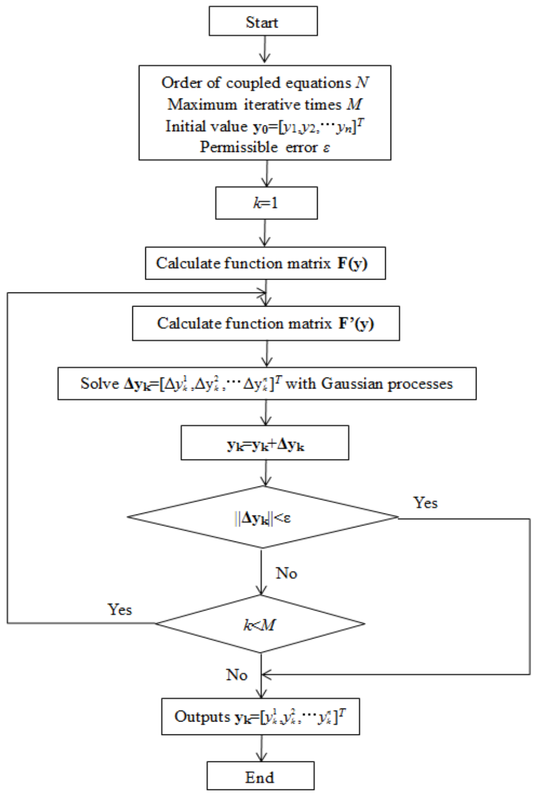

Fig. 4 Calculation flow chart of non-linear equation (set)

4. Verification of semi-analytical solution

4.1 Degeneration to the classical same modulus solution

According to the classical same modulus theory, we have $E_c=E_t=E$, $\mu_c=\mu_t=\mu$. The governing equation of the stress function will be written as

$$r^2\frac{d^2\psi}{dr^2}+r\frac{d\psi}{dr}-\psi+\frac{\alpha E}{2(1+\mu)}\frac{T_0r}{\ln(b/a)}=0 \tag{25}$$

By solving Eq. (25), the expression of the stress function containing unknown parameters can be deduced. Substituting the expression into Eq. (7), we have the stress expressions. Finally, according to the boundary conditions of Eq. (20a) and Eq. (20f), the unknown parameters can be solved and the stress expressions are written as below.

$$\sigma_{rr}=-\frac{E\alpha T_0}{2(1-\mu)}\left[\frac{\ln(b/r)}{\ln(b/a)}-\frac{(b/r)^2-1}{(b/a)^2-1}\right] \tag{26a}$$

$$\sigma_{\theta\theta}=-\frac{E\alpha T_0}{2(1-\mu)}\left[\frac{\ln(b/r)-1}{\ln(b/a)}+\frac{(b/r)^2+1}{(b/a)^2-1}\right] \tag{26b}$$

$$\sigma_{zz}=-\frac{E\alpha T_0}{2(1-\mu)}\left[\frac{2\ln(b/r)-1}{\ln(b/a)}+\frac{2}{(b/a)^2-1}\right] \tag{26c}$$

The stress expressions shown in Eq. (26) are the same as the results adopting the classical same modulus theory. That is to say, the semi-analytical solution using the bi-modulus theory can be totally degenerated to the classical same modulus solution, which partly verifies the validity and rationality of the semi-analytical method in this paper.

4.2 Numerical analysis by developing a new calculation procedure

A numerical procedure, based on UMAT, User Subroutine, ABAQUS, is developed in this paper to study the stress field of the bi-modulus cylinder. The main purpose of the procedure is to continually update the Jacobian matrix, the increments of stresses and strains in each step and stresses at the end of each step (Zhuang 2009). The principle in detail is as below.

Subjected to a temperature field, the total strain increment of the cylinder can be written as

$$d\boldsymbol{\varepsilon} = d\boldsymbol{\varepsilon}^{\mathbf{e}} + d\boldsymbol{\varepsilon}^{\mathbf{T}} \tag{27}$$

where $d\boldsymbol{\varepsilon}$ is the total strain increment, $d\boldsymbol{\varepsilon}^{\mathbf{e}}$ is the elastic strain increment and $d\boldsymbol{\varepsilon}^{\mathbf{T}}$ is the thermal strain increment as below

$$d\boldsymbol{\varepsilon} = \begin{bmatrix} d\varepsilon_{11} & d\varepsilon_{22} & d\varepsilon_{33} & d\gamma_{12} & d\gamma_{23} & d\gamma_{31} \end{bmatrix}^T \tag{28}$$

$$d\boldsymbol{\varepsilon}^{\mathbf{e}} = \begin{bmatrix} d\varepsilon_{11}^e & d\varepsilon_{22}^e & d\varepsilon_{33}^e & d\gamma_{12}^e & d\gamma_{23}^e & d\gamma_{31}^e \end{bmatrix}^T \tag{29}$$

$$d\boldsymbol{\varepsilon}^T = \begin{bmatrix} \alpha dT & \alpha dT & \alpha dT & 0 & 0 & 0 \end{bmatrix}^T \tag{30}$$

Define the stress increments of the cylinder in three directions as

$$d\boldsymbol{\sigma} = \begin{bmatrix} d\sigma_{11} & d\sigma_{22} & d\sigma_{33} & d\tau_{12} & d\tau_{23} & d\tau_{31} \end{bmatrix}^T \tag{31}$$

Then relationship between the stress increment and strain in the elastic stage can be derived

$$d\boldsymbol{\sigma} = \mathbf{D} \cdot d\boldsymbol{\varepsilon}^{\mathbf{e}} + d\mathbf{D} \cdot \boldsymbol{\varepsilon}^{\mathbf{e}} = \mathbf{D} \cdot \left(d\boldsymbol{\varepsilon} - d\boldsymbol{\varepsilon}^{\mathbf{T}} \right) + d\mathbf{D} \cdot \left(\boldsymbol{\varepsilon} - \boldsymbol{\varepsilon}^{\mathbf{T}} \right) \tag{32}$$

where $\mathbf{D}$ is the elastic constant matrix which is also defined as the Jacobian matrix

$$\mathbf{D} = \begin{bmatrix} d_{11} & d_{12} & d_{13} & 0 & 0 & 0 \\ d_{21} & d_{22} & d_{23} & 0 & 0 & 0 \\ d_{31} & d_{32} & d_{33} & 0 & 0 & 0 \\ 0 & 0 & 0 & G & 0 & 0 \\ 0 & 0 & 0 & 0 & G & 0 \\ 0 & 0 & 0 & 0 & 0 & G \end{bmatrix} \tag{33}$$

$$d_{ij} = \begin{cases} \dfrac{E_i}{-1+\mu_1\mu_2+\mu_2\mu_3+\mu_1\mu_3+2\mu_1\mu_2\mu_3}\left(-1+\prod_{j=1}^{3}\mu_j \middle/ \mu_i\right) & (i, j = 1,2,3 \text{ and } i = j) \\ \dfrac{-E_i}{-1+\mu_1\mu_2+\mu_2\mu_3+\mu_1\mu_3+2\mu_1\mu_2\mu_3}\left(\mu_j+\prod_{j=1}^{3}\mu_j \middle/ \mu_i\right) & (i, j = 1,2,3 \text{ and } i \neq j) \end{cases} \tag{34}$$

where E_1,E_2,E_3,μ_1, μ_2, μ_3 are determined according to the signs of principal stresses σ_{11},σ_{22},σ_{33}. In detail, for example, if a principal stress is positive, the elastic parameters in that direction are tensile modulus E_t, tensile Poisson's ratio μ_t, respectively. If the principle stress is negative, the elastic parameters in that direction are compressive modulus E_c, compressive Poisson's ratio μ_c, respectively. The elastic parameters meet $\mu_c/\mu_t=E_c/E_t$.

The accelerating convergence factor η (Liu and Zhang 2000, Liu and Meng 2002), the ratio of the sum of positive principal stresses to the sum of the absolute value of the three principal stresses, is introduced to define the shear modulus. For instance:

if $\sigma_{11} > 0$, $\sigma_{22} > 0$, $\sigma_{33} < 0$, then $\eta = \dfrac{\sigma_{11} + \sigma_{22}}{\sigma_{11} + \sigma_{22} + |\sigma_{33}|}$

if $\sigma_{11} > 0$, $\sigma_{22} < 0$, $\sigma_{33} < 0$, then $\eta = \dfrac{\sigma_{11}}{\sigma_{11} + |\sigma_{22}| + |\sigma_{33}|}$

if $\sigma_{11} > 0$, $\sigma_{22} > 0$, $\sigma_{33} > 0$, then $\eta = 1$

if $\sigma_{11} < 0$, $\sigma_{22} < 0$, $\sigma_{33} < 0$, then $\eta = 0$

Hence, the range of η is 0 to 1.

And then the shear modulus will be

$$G = \frac{\eta E_t + (1-\eta) E_c}{2\eta(1+\mu_t) + 2(1-\eta)(1+\mu_c)} \tag{35}$$

Since E_c, E_t, μ_c, μ_t and α will not change throughout the whole loading process, we have

$$d\mathbf{D} = \mathbf{0} \tag{36}$$

Substituting Eq. (36) into Eq. (32), we can get

$$\begin{bmatrix} d\sigma_{11} \\ d\sigma_{22} \\ d\sigma_{33} \\ d\tau_{12} \\ d\tau_{23} \\ d\tau_{31} \end{bmatrix} = \begin{bmatrix} d_{11} & d_{12} & d_{13} & 0 & 0 & 0 \\ d_{21} & d_{22} & d_{23} & 0 & 0 & 0 \\ d_{31} & d_{32} & d_{33} & 0 & 0 & 0 \\ 0 & 0 & 0 & G & 0 & 0 \\ 0 & 0 & 0 & 0 & G & 0 \\ 0 & 0 & 0 & 0 & 0 & G \end{bmatrix} \begin{bmatrix} d\varepsilon_{11} - \alpha T \\ d\varepsilon_{22} - \alpha T \\ d\varepsilon_{33} - \alpha T \\ d\gamma_{12} \\ d\gamma_{23} \\ d\gamma_{31} \end{bmatrix} \tag{37}$$

In the numerical procedure, five parameters, including E_t, μ_t, E_c, μ_c and α, are defined and a status variable is set to store and update the increment of the thermal strain at the end of each incremental step. By updating the Jocabian matrix continuously and the stresses at the end of each incremental step, the stress field in the cylinder will be gained at last. The calculation flow chart is shown as Fig. 5.

4.3 Numerical analysis by adopting the common FEM software

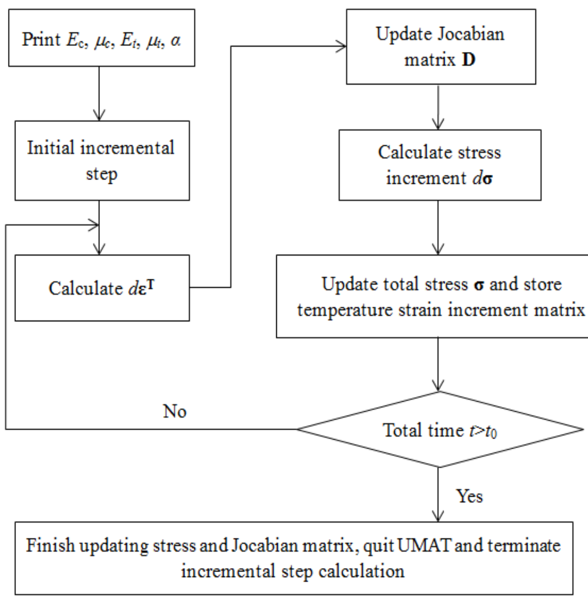

Fig. 5 Calculation flow chart of temperature stress in the cylinder

Fig. 6 Structural model in ABAQUS

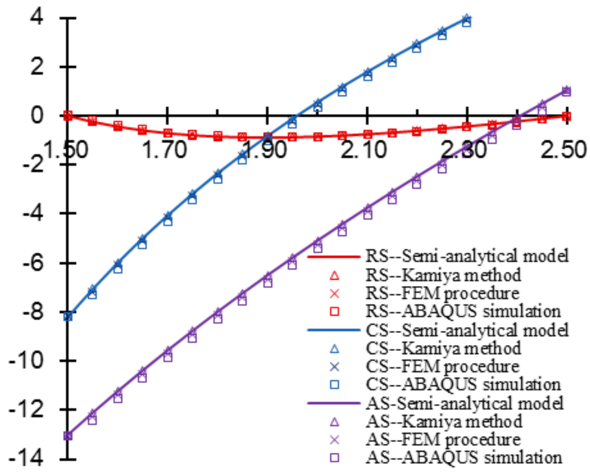

Fig. 7 Distribution of stress when E_c/E_t=1 (case I)

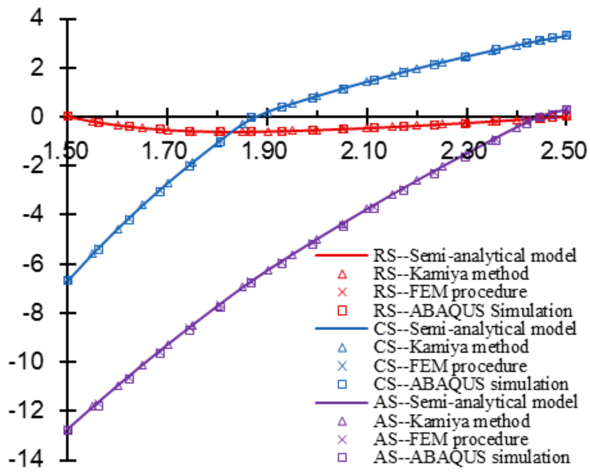

Fig. 8 Distribution of stress when E_c/E_t=2 (case I)

As is shown in Fig. 6, regard the bi-modulus cylinder as an orthotropic structure and build the 3D cylinder model with a length more than ten times the outer radius in ABAQUS. Divide the cylinder into three continuous parts according to the radius r. The initial boundary radii s_1 and s_2 are calculated according to the classical same modulus theory. E_c and E_t are determined on the basis of the sign of the stress in each direction in different parts. A steady temperature field is set in the cylinder. Considering that it is hard to simulate the mechanical response of a cylinder with infinite length, the cylinder in this paper is fixed at its ends in order to calculate accurately the axial stress. Finally,

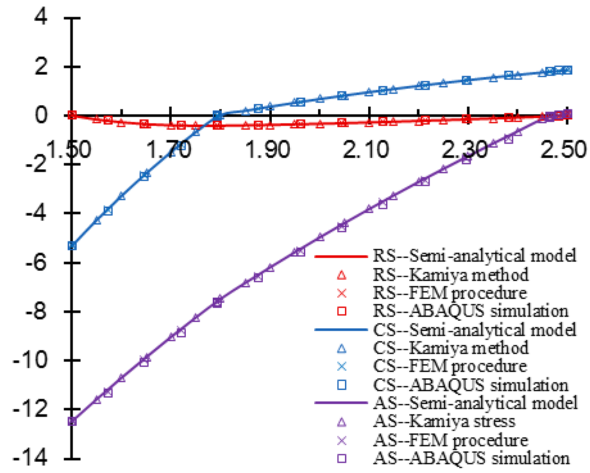

Fig. 9 Distribution of stress when E_c/E_t=4 (case I)

execute the calculation. By constantly updating the boundary radii and re-dividing regions in the cylinder after each calculation, the accurate stress field in cylinder can be gradually approached and finally obtained.

4.4 Examples validation

Consider a bi-modulus cylinder shown in Fig. 2, and the dimensions of the cylinder are a=1.5 m, b=2.5 m respectively. And the material parameters are as below: tensile modulus E_t, compressive modulus E_c, tensile Poisson's ratio μ_t, compressive Poisson's ratio μ_c, coefficient of thermal expansion $\alpha=8\times10^{-6}$/℃. The temperature at the inner wall of the cylinder is T_0=60℃.

The bi-modulus property is considered as the following two cases: (1) $E_c=2.4\times10^7$ kN/m^2, E_c/E_t=1/5~5; (2) $\bar{E}=(E_c/E_t)/2=2.4\times10^7$ kN/m^2, E_c/E_t =1/5~5.

Using the classical same modulus theory, the semi-analytical method proposed in this paper, the semi-analytical method proposed by Kamiya (1977), the FEM numerical calculation procedure, and the FEM software ABAQUS simulation method, the location of the neutral layer and the temperature stress field in the cylinder are obtained as shown in Table 1 and Figs. 7-9 (partial results list only).

5. Discussion

5.1 Advantage of the semi-analytical solution in this paper

As shown in Table 1, the semi-analytical solution derived in this paper adopting the bi-modulus theory can be completely returned to the solution using the classical same modulus theory. Simultaneously, as shown in Table 1 and Figs. 7-9, the results calculated by using the semi-analytical model in this paper is consistent with the results that gained according to Kamiya's method and ABAQUS simulation. The computational error is less than 3% which is acceptable. The error may be due to the iterative process and the round-off error. In consequence, the validity and

Table 1 The results of neutral layer location and stress of cylinder under axisymmetric temperature effect

Case I	Analytical solution by the method in this paper			Analytical solution by Kamiya's model			Numerical solution by the FEM procedure			Numerical solution by the FEM software simulation		
E_c/E_t	1	3	5	1	3	5	1	3	5	1	3	5
$E_c(\times10^7\text{kN/m}^2)$	2.4	2.4	2.4	2.4	2.4	2.4	2.4	2.4	2.4	2.4	2.4	2.4
$E_t(\times10^7\text{kN/m}^2)$	2.4	0.8	0.48	2.4	0.8	0.48	2.4	1.2	0.8	2.4	1.2	0.8
r (m)	1.5	1.5	1.5	1.5	1.5	1.5	1.5	1.5	1.5	1.5	1.5	1.5
s_1(m)	1.95814	1.82412	1.77040	1.95814	1.82412	1.77040	1.95814	1.82412	1.77040	1.95814	1.82412	1.77040
s_2(m)	2.40611	2.45601	2.47062	2.40611	2.45601	2.47062	2.40611	2.45601	2.47062	2.40611	2.45601	2.47062
σ_{rr}(MPa)	0	0	0	0	0	0	0	0	0	0	0	0
$\sigma_{\theta\theta}$(MPa)	-8.20017	-5.86612	-4.91194	-8.20045	-5.86666	-4.91253	-8.20066	-5.86659	-4.91221	-8.20106	-5.86701	-4.91263
σ_{zz}(MPa)	-12.9960	-12.5759	-12.4041	-12.9956	-12.5751	-12.4036	-12.9993	-12.5792	-12.4074	-13.0012	-12.5823	-12.4100
Case II	Analytical solution by the method in this paper			Analytical solution by Kamiya's model			Numerical solution by the FEM procedure			Numerical solution by the FEM software simulation		
E_c/E_t	1	3	5	1	3	5	1	3	5	1	3	5
$E_c(\times10^7\text{kN/m}^2)$	2.4	3.6	4.0	2.4	3.6	4.0	2.4	3.6	4.0	2.4	3.6	4.0
$E_t(\times10^7\text{kN/m}^2)$	2.4	1.2	0.8	2.4	1.2	0.8	2.4	1.2	0.8	2.4	1.2	0.8
r (m)	2.5	2.5	2.5	2.5	2.5	2.5	2.5	2.5	2.5	2.5	2.5	2.5
s_1(m)	1.95814	1.81981	1.77040	1.95814	1.81981	1.77040	1.95814	1.81981	1.77040	1.95814	1.81981	1.77040
s_2(m)	2.40611	2.43138	2.47062	2.40611	2.43138	2.47062	2.40611	2.43138	2.47062	2.40611	2.43138	2.47062
σ_{rr}(MPa)	0	0	0	0	0	0	0	0	0	0	0	0
$\sigma_{\theta\theta}$(MPa)	5.84861	3.83295	2.82717	5.84851	3.83289	2.82723	5.84869	3.83304	2.82785	5.84872	3.83310	2.82756
σ_{zz}(MPa)	1.05275	0.34497	0.16963	1.05271	0.34491	0.16960	1.05279	0.34506	0.16997	1.05281	0.34500	0.16979

rationality of the semi-analytical method in this paper have been verified.

Comparing to the semi-analytical method proposed by Kamiya (1977), the semi-analytical method in this paper simplifies the eight unknown parameters into two unknown radii of the curvature of the neutral layer. Observing coefficients in each expression of stress, we can find that the magnitude of zero-dimensional values in complex expressions relatively approaches to 1, which brings the great convenience and saves a large amount of time in calculation. Besides, this method can be easily extended to analyze the mechanical behavior of bi-modulus cylinder structures in practical engineering like civil engineering, nuclear engineering (Li *et al*. 2008, Fang *et al*. 2014).

5.2 Advantage of the FEM procedure in this paper

As shown in Table 1 and Figs. 7-9, the results gained by FEM procedure are in great consistence with the results obtained by the semi-analytical methods and ABAQUS simulation. Acceptable computational errors less than 3% can be found in all kinds of examples, which may be caused by the grid density, the iterative process, the round-off error of terminal value. Hence, the FEM procedure is verified to be rational and accurate.

The FEM procedure has two advantages. First, the FEM procedure can simplify the modeling process. For the FEM software simulation, since the bi-modulus property of materials cannot be defined, initial boundary radii are required to be calculated by considering the same structural model with the same elastic modulus. And then complex iteration processes to seek new boundary radii are carried out continuously until the accurate boundary radii are finally obtained. However, the FEM procedure can calculate directly the boundary radii, which means that users merely need to establish one model. Therefore, the modeling process is greatly simplified. Second, the FEM procedure can calculate the mechanical behavior of bi-modulus structures with complex geometry and boundary conditions and subjected to complex loads. It is well known that the analytical methods can only be applied when a simplified model from an engineering structure is obtained. Simultaneously, for the FEM software simulation, it can only be used when the initial neutral layer location is gained. In consequence, for complex engineering models, the analytical methods and the FEM software simulation will both have their own limitation, which makes the FEM procedure stand out.

5.3 Distribution of radial stress

As shown in Figs. 10-12, when the tensile modulus and the compressive modulus change, comparing to the circumferential stress and the axial stress, although the radial stress in the cylinder varies more obviously, it maintains in a small magnitude. Therefore, the effect of the bi-modulus property on the radial stress can be ignored in the structural design.

5.4 Distribution of axial stress

As shown in Fig. 11, for the axial stress, the neutral layer location shows little variation with the alteration of the tensile modulus and the compressive modulus. Consequently, the classical same modulus theory can be extended to the qualitative analysis of the axial stress in the

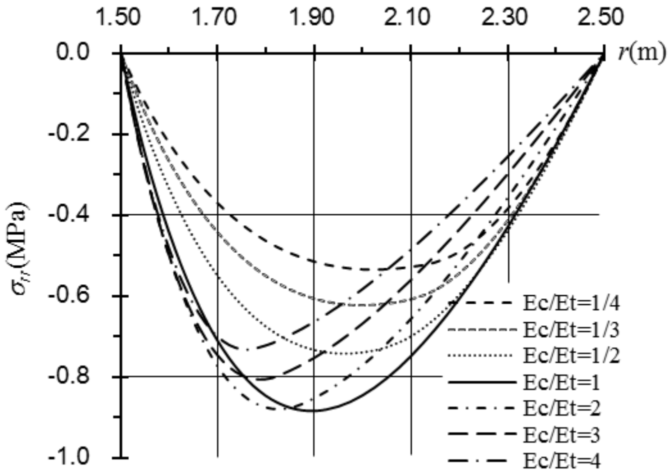

Fig. 10 Distribution of radial stress (case II)

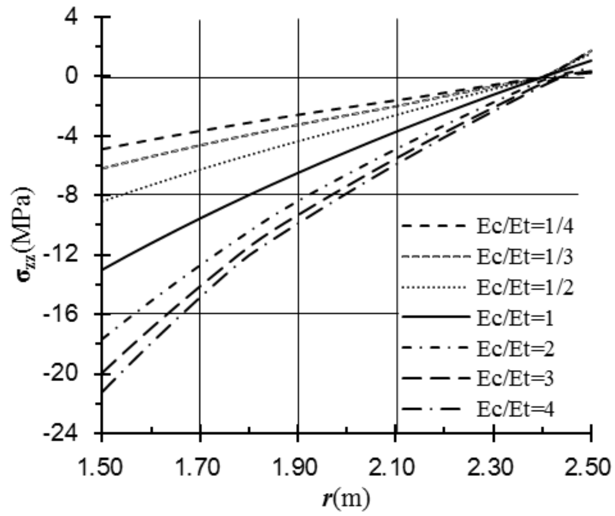

Fig. 11 Distribution of axial stress (case II)

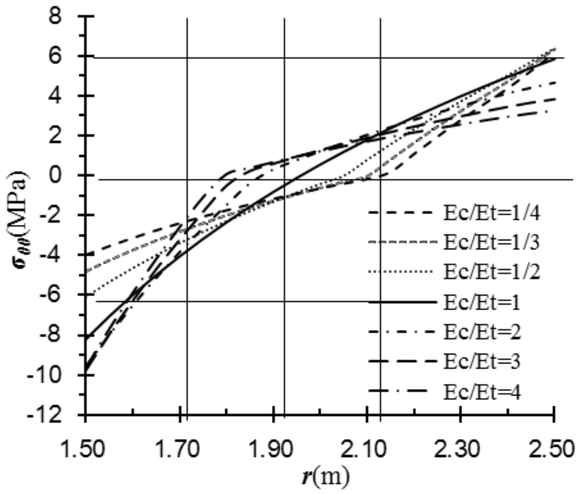

Fig. 12 Distribution of circumferential stress (case II)

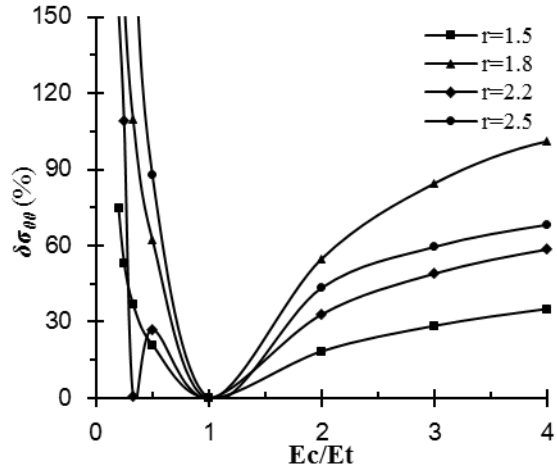

Fig. 13 Computational error of circumferential stress between two theories (case I)

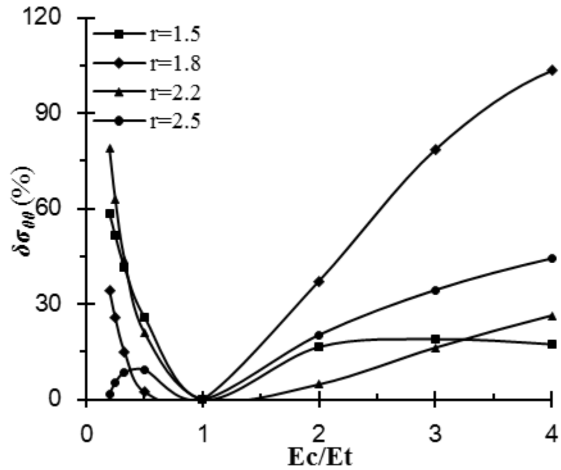

Fig. 14 Computational error of circumferential stress between two theories (case II)

cylinder when the structural design is conducted.

5.5 Distribution of circumferential stress

As depicted in Fig. 12, considering the circumferential stress in the cylinder, the neutral layer location changes distinctly as the tensile modulus and the compressive modulus alter. When $E_c > E_t$, with the increase of E_c/E_t, the neutral layer moves toward the inner wall of the cylinder. The tensile region will enlarge and the compressive region will correspondingly diminish with a gradually decreasing rate. For the concrete widely used in civil engineering, the tensile region will extend because of the bi-modulus property. If the classical same modulus theory is still adopted, the crack may increase in the concrete cylinder, which may have an adverse effect on the normal operation of such structure.

5.6 Computational error of stress between bi-modulus and same modulus theory

According to the analysis above, the circumferential stress should be paid enough attention to when designing cylinder structures composed of bi-modulus materials. As shown in Figs. 13-14, the computational error of the circumferential stress between the bi-modulus theory and the classical same modulus theory increases as the

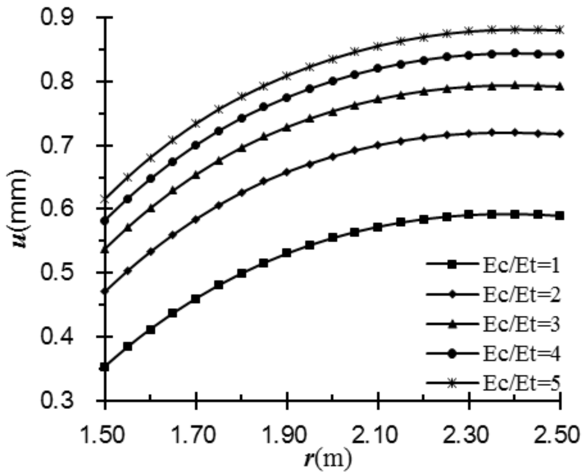

Fig. 15 Response of radial displacement (case II)

difference between the tensile modulus and the compressive modulus magnifies.

For the concrete material, the ratio of the compressive modulus to the tensile modulus is approximately 2.5. The maximum computational error between two theories is about 70%. Hence, a large amount of concrete may be saved if the bi-modulus theory is introduced into the structural design of the cylinder.

5.7 Radial displacement

As shown in Fig. 15, keep the total stiffness of the cross -section constant and change the value of E_c/E_t. The displacement of the cylinder increases as E_c/E_t increases. It indicates that when the bi-modulus property is considered, comparing to the classical same modulus theory, the displacement increases as a result of the non-uniformity of the cross-section stiffness, which means that the resistance to the deformation of the cylinder decreases.

6. Conclusions

In this paper, a stress function is introduced to modify the existing semi-analytical method to calculate the axisymmetric temperature stress in the bi-modulus thick cylinder, which simplifies the calculation process and increases the calculation velocity and is easier to be used to study the influence of the bi-modulus property of materials on the mechanical response of structures in the practical engineering. Meanwhile, a numerical procedure is developed to calculate the temperature stress in bi-modulus structures, which simplifies the modeling process of a bi-modulus structure and can be extended to analyze the temperature stresses of bi-modulus structures with arbitrary geometric shapes and complex boundary conditions. Finally, some rational suggestions on qualitative analysis and quantitative design of such structure are proposed as follows.

- Comparing with the circumferential stress and the axial stress, the radius stress changes with a small magnitude after the bi-modulus property of materials is considered. The influence of the bi-modulus property on the radial stress can be ignored in the design of the bi-modulus cylinder.
- The location of the neutral layer shows little variation when the difference between the tensile modulus and the compressive modulus enlarges. The classical same modulus theory can still be adopted to execute the qualitative analysis of the axial stress in the design of the bi-modulus cylinder.
- When the bi-modulus property is considered in the structural design of the cylinder, the key problem is to analyze its effect on the circumferential stress distribution. For the concrete widely used in engineering, tensile region will extend and more cracks may appear when the bi-modulus property is considered. The tensile stress will decrease approximately 70% in maximum comparing to the result gained by the classical same modulus theory. Rationally choosing the strength grade of concrete may excavate the potential of the mechanical property of materials and avoid the excessive consumption of materials.
- The bi-modulus property of materials will lead to the increase of the discreteness of the structural stiffness and the decrease of the resistance to the external force and the deformation.

Acknowledgments

We acknowledge the support of the National Natural Science Foundation of China (11072143 and 11272200).

Peikui Huang especially thanks for the support by the Graduate Student Overseas Study Program of South China Agricultural University (Grant NO.2017LHPY001).

References

Ambartsumyan, C.A., Wu, R.F. and Zhang, Y.Z. (1986), *Different Modulus of Elasticity Theory*, China Railway Publishing House, China.

Bertoldi, K., Bigoni, D. and Drugan, W. J. (2008), "Nacre: An orthotropic and bimodular elastic material", *Compos. Sci. Technol*., **68**(6), 1363-1375.

Chandrashekhara, K. and Bhimaraddi, A. (1982), "Elasticity solution for a long circular sandwich cylindrical shell subjected to axisymmetric load", *Int. J. Solid. Struct*., **18**(7), 611-618.

Fang, X., Yu, S.Y., Wang, H.T. and Li, C.F. (2014), "The mechanical behavior and reliability prediction of the HTR graphite component at various temperature and neutron dose ranges", *Nucl. Eng. Des*., **276**(2), 9-18.

Geim, A.K. (2009), "Graphene: status and prospects", *Sci.*, **324**(5934), 1530-1534.

Gilbert, G.N.J. (1961), "Stress/strain properties of cast iron and Poisson's ratio in tension and compression", *Brit. Cast Res. Assn. J*., **9**, 347-363.

Green, A.E. and Mkrtichian, J.Z. (1977), "Elastic solids with different moduli in tension and compression", *J. Elasticity*, **7**(4), 369-386.

Guo, Z.H. and Zhang, X.Q. (1987), "Investigation of complete stress-deformation curves for concretes in tension", *ACI Mater. J*., **84**(4), 278-285.

He, X.T., Chen, Q., Sun, J.Y. and Chen, S.L. (2010), "Application of Kirchhoff hypotheses to bending thin plates with different moduli in tension and compression", *J. Mech. Mater. Struct*. **5**(5), 755-769.

He, X.T., Chen, Q., Sun, J.Y. and Zheng, Z.L. (2012), "Large-deflection axisymmetric deformation of circular clamped plates with different moduli in tension and compression", *Int. J. Mech. Sci*., **62**(1), 103-110.

He, X.T., Chen, S.L. and Sun, J.Y. (2007), "Applying the equivalent section method to solve beam subjected to lateral force and bend-compression column with different moduli", *Int. J. Mech. Sci.*, **49**(7), 919-924.

He, X.T., Hu, X.J., Sun, J.Y. and Zheng, Z.L. (2010), "An analytical solution of bending thin plates with different moduli in tension and compression", *Struct. Eng. Mech*., **36**(3), 363-380.

He, X.T., Xu, P., Sun, J.Y. and Zheng, Z.L. (2015), "Analytical solutions for bending curved beams with different moduli in tension and compression", *Mech. Adv. Mater. Struct*., **22**(5), 325-337.

He, X.T., Zheng, Z.L., Sun, J.L., Li, Y.M. and Chen, S.L. (2009), "Convergence analysis of a finite element method based on different moduli in tension and compression", *Int. J. Solid. Struct*., **46**(20), 3734-3740.

Jones, R.M. (1971), "Buckling of circular cylindrical shells with different moduli in tension and compression", *AIAA J*., **9**(1), 53-61.

Jones, R.M. (1971), "Buckling of stiffened multilayered circular cylindrical shells with different orthotropic moduli in tension and compression", *AIAA J*., **9**(5), 917-923.

Kamiya, N. (1977), "Thermal stress in a bi-modulus thick cylinder", *Nucl. Eng. Des*., **40**, 383-391.

Leal, A.A., Deitzel, J.M. and Gillespie, Jr J.W. (2009), "Compressive strength analysis for high performance fibers with different modulus in tension and compression", *J. Compos. Mater*., **43**(6), 661-674.

Li, H., Fok, S.L. and Marsden, B. J. (2008), "An analytical study on the irradiation-induced stresses in nuclear graphite moderator bricks", *J. Nucl. Mater*., **372**(2-3), 164-170.

Liu, X.B. and Meng, Q.C. (2002), "On the convergence of finite element method with different extension-compression elastic modulus", *J. Beijing Univ. Aeronaut. Astronaut*., **28**(2), 232-234.

Liu, X.B.and Zhang, Y.Z. (2000), "Modulus of elasticity in shear and accelerate convergence of different extension-compression elastic modulus finite element method", *J. Dalian Univ. Technol*., **40**(5), 527-530.

Medri, G. (1982), "A nonlinear elastic model for isotropic materials with different behavior in tension and compression", *J. Eng. Mater. Technol*., **16**(104), 26-28.

Patel, B.P., Khan, K. and Nath, Y. (2014), "A new constitutive model for bimodular laminated structures: Application to free vibrations of conical/cylindrical panels", *Compos. Struct*., **110**, 183-191.

Shapiro, G.S. (1971), "Deformation of bodies with different tensile and compressive strengths (stiffnesses)", *Mech. Solid*., **22**(5), 82-89.

Shi, J. and Gao, Z.L. (2015), "Ill-loaded layout optimization of bi-modulus material", *Finite Elem. Anal. Des*., **95**, 51-61.

Shi, J., Cai, K. and Qin, Q.H. (2014), "Topology optimization for human proximal femur considering bi-modulus behavior of cortical bones", *MBC: Mol. Cell. Biomech*., **11**(4), 235-248.

Timoshenko, S. (1941), *Strength of Materials, Part II: Advanced Theory and Problems*, 2nd Edition, Van Nostrand , USA.

Tsoukleri, G., Parthenios, J., Papagelis, K., Jalil, R., Ferrari, A.C., Geim, A.K., ... and Galiotis, C. (2009), "Subjecting a graphene monolayer to tension and compression", *Small*, **5**(21), 2397-2402.

Vijayakumar, K. and Rao, K P. (1987), "Stress-strain relation for composites with different stiffnesses in tension and compression", *Comput. Mech*., **2**(3), 167-175.

Wu, X., Yang, L.J., Huang, C. and Sun, J. (2010), "Large deflection bending calculation and analysis of bi-modulus rectangular plate", *Eng. Mech*., **27**(1), 17-22.

Yang, H.T. and Zhu, Y.L. (2006), "Solving elasticity problems with bi-modulus via a smoothing technique", *Chin. J. Comput. Mech*., **23**(1), 19-23.

Yang, H.T., Wu, R.F., Yang, K.J. and Zhang, Y.Z. (1992), "Solution to problem of dual extension-compression elastic modulus with initial stress method", *J. Dalian Univ. Technol*., **32**(1), 35-39.

Yao, W.J. and Ma, J.W. (2013), "Semi-analytical buckling solution and experimental study of variable cross-section rod with different moduli", *J. Eng. Mech. Div*., ASCE, **139**(9), 1149-1157.

Yao, W.J. and Ye, Z.M. (2004), "Analytical solution for bending beam subject to lateral force with different modulus", *J. Appl. Math. Mech. (Engl. Transl.)*, **25**(10), 1107-1117.

Yao, W.J. and Ye, Z.M. (2004), "Analytical solution of bending-compression column using different tension-compression modulus", *J. Appl. Math. Mech. (Engl. Transl.)*, **25**(9), 983-993.

Yao, W.J. and Ye, Z.M. (2006), "Internal forces for statically indeterminate structures having different moduli", *J. Eng. Mech. Div*., ASCE, **132**(7), 739-746.

Yao, W.J., Ma, J.W., Gao, J.L. and Qiu, Y.Z. (2015), "Nonlinear large deflection buckling analysis of compression rod with different moduli", *Struct. Eng. Mech*., **54**(5), 855-875.

Yao, W.J., Zhang, C.H. and Jiang, X.F. (2006), "Nonlinear mechanical behavior of combined members with different moduli", *Int. J. Nonlin. Sci. Numer. Simul*., **7**(2), 233-238.

Ye, Z.M., Yu, H.G. and Yao, W.J. (2001), "A new elasticity and finite element formulation for different Young's modulus when tension and compression loading", *J. Shanghai Univ*., **5**(2), 89-92.

Ye, Z.M., Yu, H.R. and Yao, W.Y. (2001), "A finite element formulation for different Young´s modulus when tension and compression loading", *Combinational and Computational Mathematics Center Conference on Computational Mathematics, Pohang University of Science and Technology*, South Korea.

Zhang, Y.Z. and Wang, Z.F. (1989), "The finite element method for elasticity with different moduli in tension and compression", *Chin. J. Comput. Mech*., **6**(1), 236-246.

Zhou, J.G. (1981), "Method of calculating the temperature stresses in composite hollow cylinder", *J. Build. Struct*., **3**, 42-55.

Zhuang, Z. (2009), Finite element analysis and application based on ABAQUS, Tsinghua University Press, Beijing, China.

CC